ISTITUTO NAZIONALE DI FISICA NUCLEARE
Laboratori Nazionali di Frascati

LNF-84/13

G.Battistoni et al.: AN EXPERIMENTAL STUDY OF THE NEUTRINO BACKGROUND IN UNDERGROUND EXPERIMENTS ON NUCLEON DECAY

Estratto da:
Nuclear Instr. and Meth. 219, 300 (1984)

Servizio Documentazione
dei Laboratori Nazionali di Frascati
Cas. Postale 13 - Frascati (Roma)

Nuclear Instruments and Methods in Physics Research 219 (1984) 300–310
North-Holland, Amsterdam

AN EXPERIMENTAL STUDY OF THE NEUTRINO BACKGROUND IN UNDERGROUND EXPERIMENTS ON NUCLEON DECAY

G. BATTISTONI [1], E. BELLOTTI [2], G. BOLOGNA [3], P. CAMPANA [1], C. CASTAGNOLI [3], V. CHIARELLA [1], D.C. CUNDY [4], B. D'ETTORRE PIAZZOLI [3], E. FIORINI [2], E. IAROCCI [1], G. MANNOCCHI [3], G.P. MURTAS [1], P. NEGRI [2], G. NICOLETTI [1], L. PERIALE [3], P. PICCHI [3], M. PRICE [4], A. PULLIA [2], S. RAGAZZI [2], M. ROLLIER [2], O. SAAVEDRA [3], L. TRASATTI [1] and L. ZANOTTI [2]

[1] *Laboratori Nazionali dell'INFN, Frascati, Italy*
[2] *Dipartimento di Fisica dell'Università and INFN, Milano, Italy*
[3] *Istituto di Cosmogeofisica del CNR, Torino, Italy*
[4] *CERN, European Organization for Nuclear Research, Geneva, Switzerland*

Received 14 July 1983

In order to investigate experimentally the background induced by atmospheric neutrinos in nucleon decay experiments we have simulated very closely the expected spectrum by means of an accelerator produced neutrino beam and exposed to it a test module of a fine train calorimeter. Two runs have been performed with the detector axis placed at 0° and 45° with respect to the neutrino beam direction, and a total of 400 events have been detected and measured. The background induced by atmospheric neutrinos into various nucleon decay channels has been deduced from these data. These results can be applied to the present or planned nucleon decay experiments.

1. Introduction

The most elusive background and the ultimate sensitivity of nucleon decay experiments placed deep underground is due to interactions in the detector of atmospheric neutrinos whose intensity is obviously unaffected by depth [1]. If the charged secondaries of these interactions are totally contained in the detector (confined events), they can simulate nucleon decay events. This is particularly important for fine grain calorimeters, where iron or other heavy materials are used as absorbers. In fact, Fermi motion and reinteractions of charged secondaries inside nuclei play an important role in determining event topologies. Neutrinos from the sun or from gravitational collapses do not contribute to this background due to their low energies (a few MeV and a few tens of MeV, respectively).

We will discuss here the expected features of interactions by atmospheric neutrinos using the data obtained in a dedicated experiment carried out at CERN with an artificial neutrino beam similar in spectrum to that of atmospheric neutrinos.

2. Atmospheric neutrinos

Atmospheric neutrinos are generated by decay in flight of pions, kaons and muons, resulting from the interactions with the nuclei of the atmosphere by cosmic ray hadrons (mainly protons). From the prediction based on the production mechanism [2], the antineutrino flux is expected to be about 50% lower than the neutrino flux. About a third of neutrinos and antineutrinos are expected to be of the electron type. Moreover the horizontal intensity is expected to be about 30% more than the vertical one, for the energy region compatible with nucleon decay.

Unfortunately, apart from the recent results by the Kolar Gold Field [3] and Mont-Blanc [4] experiment, no data are available for interactions of atmospheric neutrinos inside an underground calorimetric detector. Most of the available information still comes from an experiment by the Case–Irvine–Witswatersrand Collaboration [5], performed at a depth of 8890 m of water equivalent of standard rock (m.w.e.), where the horizontal neutrino flux has been deduced from the number of horizontal muons, produced by interactions of muon neutrinos in the rock surrounding the detector. These muons can be discriminated from the atmospheric ones which are strongly peaked around the vertical at great depth. These results are confirmed by those of the Kolar Gold Field nucleon decay experiment, performed also at great depth (~ 7600 m.w.e.), but at a much lower geomagnetical latitude (~ 3° NL.) [3]. This introduces an average suppression of 1.6 in the atmospheric neutrino flux.

Table 1
Atmospheric neutrinos (fluxes are per m^2 and year in units of 10^{10}; events are per kiloton).

Energy (GeV)	Neutrino flux	CC events		Total events	CC events		Inel. events	Total events	Electronic CC events (total)	Neutral current energy visible	Muonic events	Muonless events	Total
		Elastic events	Inel. events		Antin. flux	Elastic events							
0.3–0.4	5.3	6.8	1.2	8.0	4.8	2.5	–	2.5	5.3	1.0	10.5	6.3	16.8
0.4–0.6	5.9	9.6	3.6	13.2	5.6	3.7	1.3	5.0	9.1	1.8	18.2	10.9	29.1
0.6–0.8	3.1	6.3	3.7	10.0	2.8	2.3	1.3	3.6	6.3	1.2	13.6	7.5	21.1
0.8–1.0	1.78	4.2	2.0	7.2	1.5	1.3	0.9	2.2	4.9	1.3	9.4	6.2	15.6
1.0–1.2	1.28	3.0	2.8	5.8	1.08	1.3	0.6	1.9	3.4	1.0	7.7	4.4	12.1
1.2–1.4	0.71	1.9	2.2	4.1	0.59	0.6	0.6	1.2	2.6	0.9	5.3	3.5	8.8
1.4–1.6	0.47	1.3	1.8	3.1	0.41	0.6	0.4	1.0	2.0	0.8	4.1	2.8	6.9
1.6–1.8	0.35	0.9	1.8	2.7	0.30	0.4	0.4	0.8	1.7	0.6	3.5	2.3	5.8
1.8–2.0	0.30	0.8	1.7	2.5	0.25	0.3	0.6	0.9	1.7	0.4	3.4	2.1	5.5
2.0–3.0	0.95	2.5	8.0	10.5	0.80	1.1	2.1	3.2	6.4	0.6	13.7	7.0	20.7
3.0–4.0	0.37	1.0	4.8	5.8	0.30	0.8	0.8	1.6	3.7	0.2	7.4	3.9	11.1
4.0–5.0	0.19	0.6	1.3	1.9	0.15	0.3	0.3	0.6	1.3	0.1	2.5	1.4	3.9
5.0–7.0	0.11	0.3	0.5	0.8	0.09	0.1	0.1	0.2	0.5	0.1	1.0	0.6	1.6
Total	20.9	39.2	36.4	75.6	18.7	15.3	9.4	24.7	48.9	10.0	110.3	58.9	169.2

Table 2
Accelerator neutrinos (fluxes are per m^2 and 10^{18} protons in units of 10^{13}; events are per ton and 10^{18} protons).

Energy	Neutrino flux	CC events		Total	CC events		Inel.	Total	ELastic	Inel.	Total	Muonless	Total
		Elastic	Inel.		Antin. Flux	Elastic							
0.3–0.4	1.72	2.2	0.4	2.6	1.70	0.9	0.1	1.0	3.1	0.5	3.6	0.4	4.0
0.4–0.6	2.94	4.8	1.8	6.6	2.10	1.4	0.5	1.9	6.2	2.3	8.5	1.0	9.5
0.6–0.8	1.92	3.9	2.3	6.2	0.87	0.7	0.4	1.1	4.6	2.7	7.3	0.7	8.0
0.8–1.0	1.87	4.4	3.2	7.6	0.67	0.6	0.4	1.0	5.0	3.6	8.6	0.6	4.2
1.0–1.2	0.89	2.3	2.1	4.4	0.34	0.4	0.2	0.6	2.7	2.3	5.0	0.6	5.6
1.2–1.4	0.55	1.5	1.7	3.2	0.27	0.3	0.3	0.6	1.8	2.0	3.8	0.5	4.3
1.4–1.6	0.39	1.1	1.5	2.6	0.20	0.3	0.2	0.5	1.4	1.7	3.1	0.4	3.4
1.6–1.8	0.30	0.8	1.5	2.3	0.14	0.2	0.2	0.4	1.0	1.7	2.7	0.3	3.0
1.8–2.0	0.26	0.7	1.5	2.2	0.08	0.1	0.2	0.3	0.8	1.7	2.5	0.3	2.8
2.0–3.0	0.72	1.9	6.1	8.0	0.15	0.2	0.4	0.6	2.1	6.5	8.6	0.7	4.3
3.0–4.0	0.34	0.9	4.4	5.3	0.04	0.1	0.1	0.2	1.0	4.5	5.5	0.3	5.8
4.0–5.0	0.17	0.3	2.9	3.4	0.02		0.1	0.1	0.5	3.0	3.5	0.1	3.6
5.0–6.0	0.04	0.1	0.9	1.0			0.1	0.1	0.1	1.0	1.1	0.1	1.2
Total	12.11	25.1	30.3	55.4	7.02	5.2	3.2	8.4	30.3	33.5	63.8	6.0	69.8

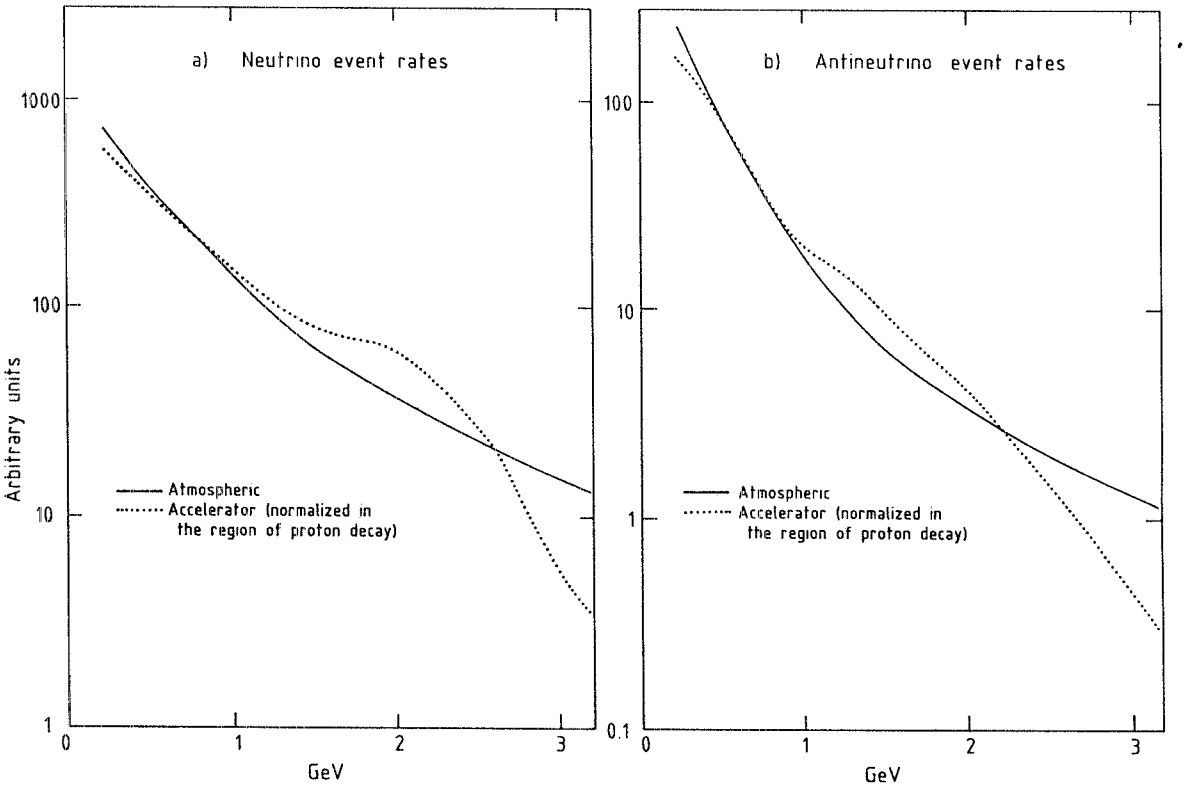

Fig. 1. Comparison of the atmospheric neutrino and antineutrino spectra with those of the beams obtained from 10 GeV protons on the bare target.

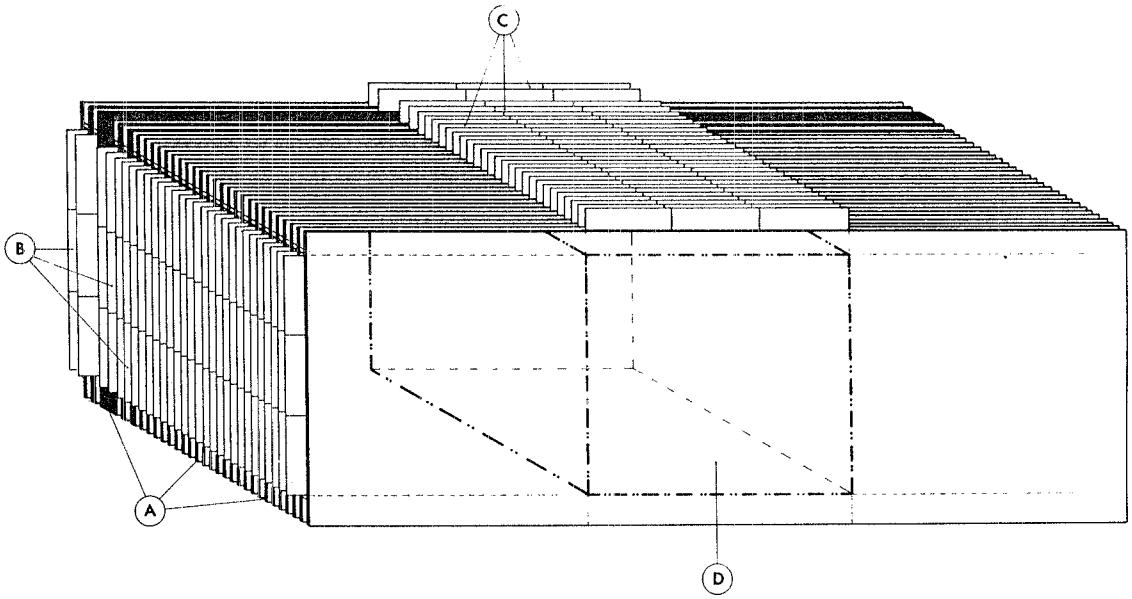

Fig. 2. A sketch of the detector used in the present experiment. (a) The vertical iron plates, (b) the detector tubes, plus the x-strips, (c) the y-strips, (d) the fiducial volume.

The neutrino fluxes at 45°N, corresponding to the Mont-Blanc and Frejus experiments, are reported in table 1. Those expected in the American experiments are approximately the same. Using the predicted fluxes we have calculated the neutrino and antineutrino event rates which are also shown in table 1. The cross sections for elastic charged current neutrino interactions have been obtained from threshold to 1.2 GeV by a fit to the data of the ANL deuterium bubble chamber [6], and taken as constant at a value of 0.45×10^{-38} cm^2/nucleon at higher energies. The cross section for single pion production in charged current neutrino interactions has been obtained from threshold to 1.2 GeV from a linear fit to the above mentioned data [7] and to the results obtained in heavy freon by the Gargamelle collaboration [8]. A constant cross section of 0.45×10^{-38} cm^2/nucleon has been taken for the same reaction at higher energies. A total cross section proportional to the neutrino energy has been taken above 1 GeV (production of more than one pion has been neglected at lower energies). The slope has been taken as 0.75×10^{-38} cm^2/GeV nucleon by averaging between the ANL [9] and Gargamelle [10] results.

Since no data are available on cross sections for elastic antineutrino interactions below 1.2 GeV, we have calculated the antineutrino data by using values of 0.84 and 0.95 GeV for the masses of the vector and axial-vector bosons which describe the form factors, respectively. For energies above 1.2 GeV we have taken a constant elastic cross section of 0.19×10^{-38} cm^2/nucleon. The cross section for charged current single pion production by antineutrinos has been obtained by fitting the freon and propane data in Gargamelle [11–13], while above 1 GeV a total cross section proportional to the antineutrino energy. The slope is taken as 0.28×10^{-38} cm^2/GeV nucleon, as given by Gargamelle [10].

The neutral current contribution has been evaluated by assuming a ratio of neutral to charged current interactions at the same hadronic energy equal to 0.15 and 0.25 for neutrinos and antineutrinos, respectively. The average hadronic energy has been taken as one half and one third of the total energy for neutrino and antineutrino interactions.

The predictions of table 1 could be in error up to 50%, at least for energies below 1 GeV, due to uncertainty in the neutrino and antineutrino fluxes and on their electronic and muonic composition, as well as uncertainty in the neutrino and antineutrino cross sections.

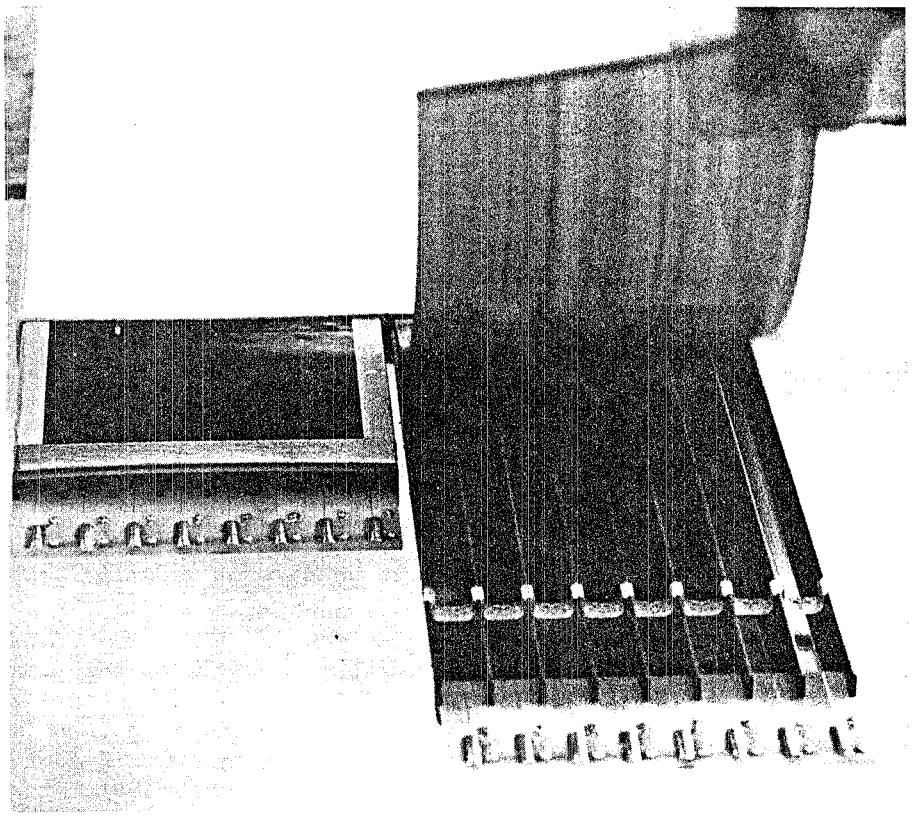

Fig. 3. Resistive tubes with bidimensional read-out.

It can be seen from table 1 that the total rate of neutrino and antineutrino interactions above 0.3 GeV amounts to about 0.16 per ton per year, and that about 20% of such interactions occur at an energy compatible with nucleon decay if a 20% energy resolution is assumed. This background can be further reduced only by discriminating neutrino interactions from genuine nucleon decay events on the basis of different kinematical properties.

3. Accelerator neutrinos

The study of the atmospheric neutrino background can be carried out experimentally taking advantage of the fact that the energy spectrum of an artificial neutrino beam produced by protons of an energy around 10 GeV impinging on the "bare" target, without any focusing of the secondary pions and kaons, is very similar to the atmospheric neutrino one.

Taking into account the beam layouts available at CERN we have adopted an unfocused neutrino beam produced by 10 GeV protons on a 60 cm long, 1.2 cm diameter cylindrical beryllium target, with a 10.0 m decay tunnel, and a detector–target distance of 23 m. The energy spectrum of this beam has been evaluated by means of the Monte-Carlo program NUBEAM [14] and is compared in fig. 1 with the one expected for atmospheric neutrinos. The expected rates of neutrino events, calculated as for those of atmospheric neutrinos, are reported in table 2. We consider them to be affected by an error of 30% due to uncertainties in the evaluation of the cross section and flux.

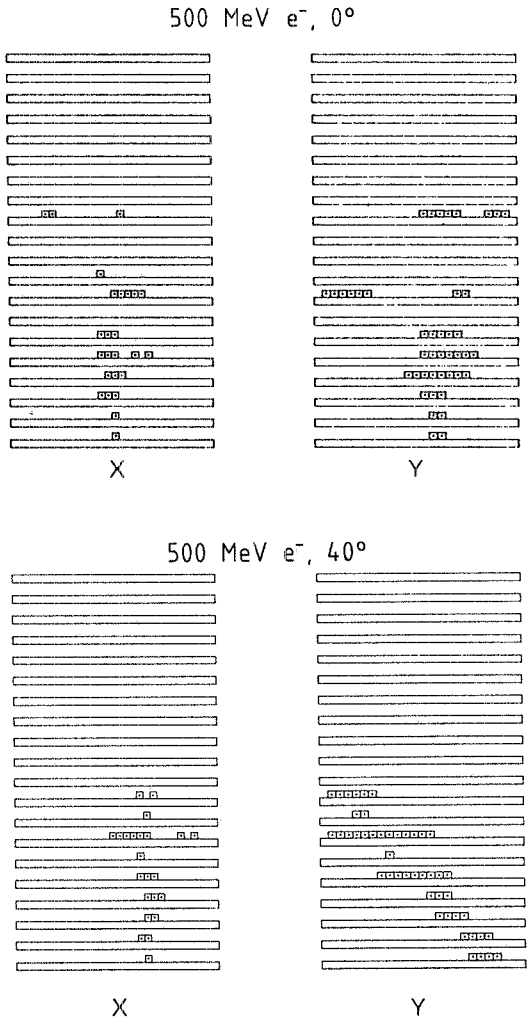

Fig. 4. A 500 MeV/c electron incident at 0° and 40° with respect to the detector axis.

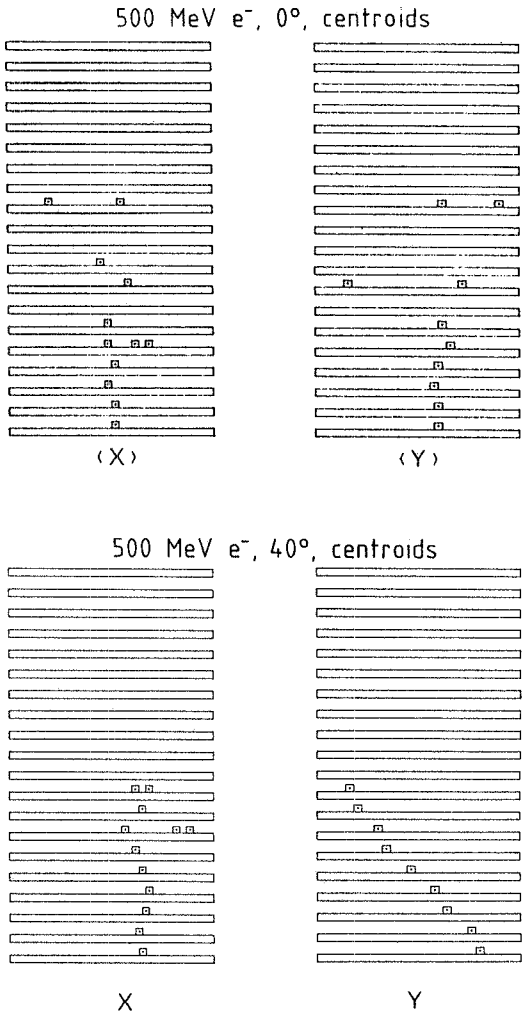

Fig. 5. The same events as fig. 4, where only the centroids are shown.

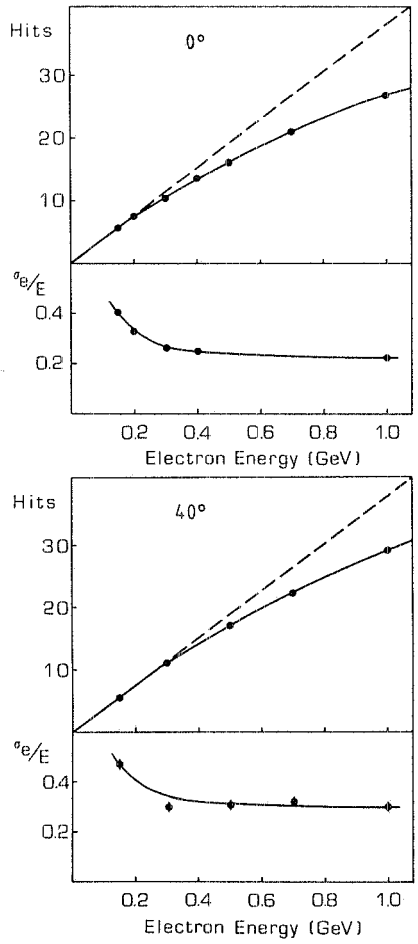

Fig. 6. Number of hits in the XZ planes and energy resolution as function of energy for electron incident at 0° and 40°.

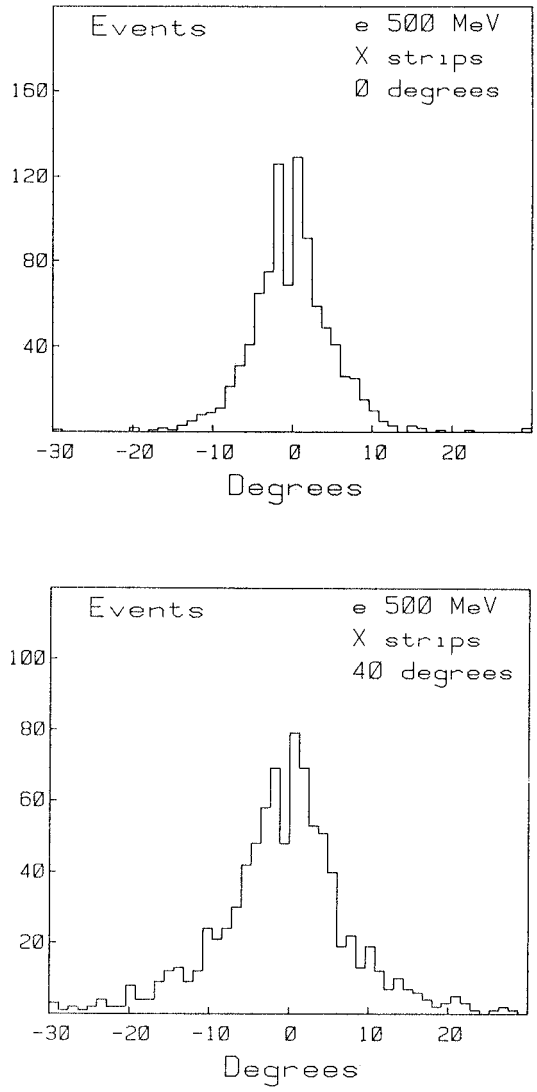

Fig. 7. Angular resolution for a 500 MeV/c electron incident at 0° and 40°.

4. The test module

The test module used in the present experiment is almost identical in structure to that of the nucleon decay detector [4–15] operating at present in the Mont-Blanc laboratory. This consists of a cube ($3.5 \times 3.5 \times 3.5$ m^3) made of 134 horizontal iron plates, 1 cm thick, 3.5 cm side, interleaved with planes of plastic streamer tubes with bidimensional read-out [16].

The test module (fig. 2) consists of 29 vertical plates of iron ($1 \times 100 \times 350$ cm^3) interleaved with planes of plastic streamer tubes identical to those of the Mont-Blanc detector (1 cm$^2 \times 350$ cm). Details of the plastic streamer tubes are visible in fig. 3. Tubes were operated with an argon + isobutane, 1 + 3 gas mixture.

Each detector plane is read out by 966 X strips (parallel to wires), 350 cm long, 0.4 cm wide, 1 cm pitch, covering the entire plane surface and by 96 Y strips (orthogonal to wires), 105 cm long, 1 cm wide and with 1.2 cm pitch, covering only the central detector area.

Signals from strips (≥ 2 mV/ 50 Ω) are fed into a monolithic amplifier discriminator circuit (LeCroy ML200). The TTL output is shaped to 6 μs. Outputs from 8 contiguous channels are then fed into an 8-bit, parallel in serial out, shift register. 32 electronic channels are grouped into a single printed circuit card. A single bus allows serial readout of the all shift registers of each plane. A single CAMAC processor (LeCroy STOS controller 4700) is connected to eight of such buses. At every trigger the processors generate the load signal to the shift registers; data are then transferred from processors to a PDP 11/40 computer without any selection.

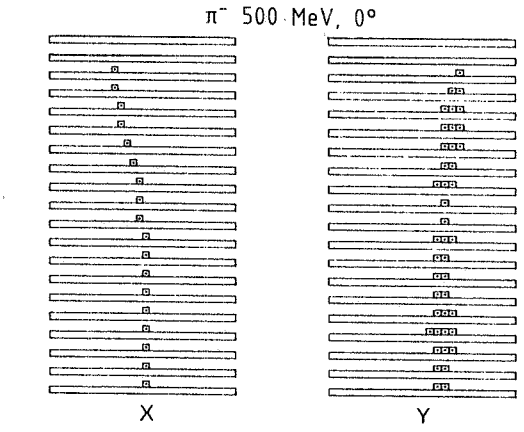

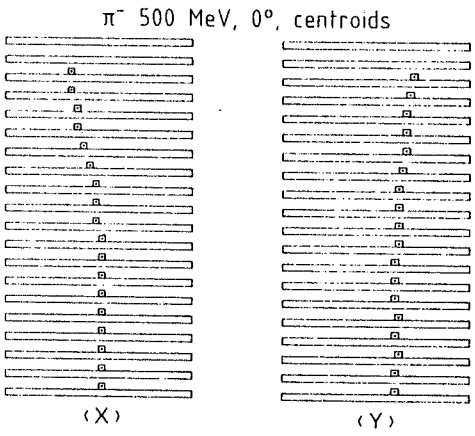

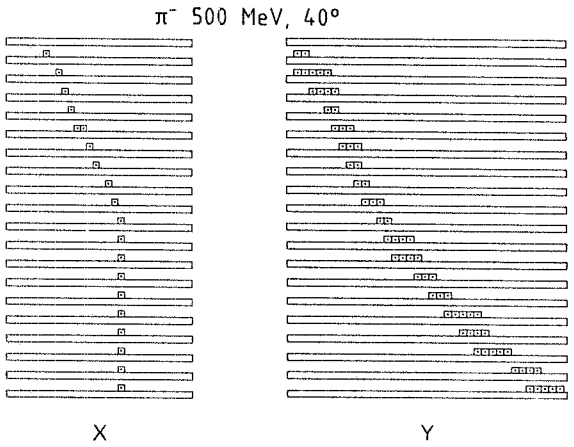

Fig. 8. A 500 MeV/c negative pion incident at 0° and 40°.

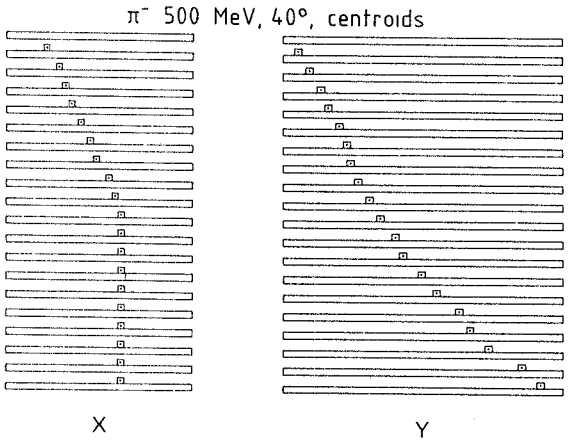

Fig. 9. Centroid distribution for the events of fig. 8.

5. Calibration to charged particles

In order to assess a priori the performance of our calorimeter to secondaries produced by neutrino interactions and nucleon decays, the test module has been exposed to various Cherenkov separated negative beams of secondary pions and electrons at the CERN PS. Runs have been carried out at momenta ranging from 0.150 to 2.0 GeV/c and with angles between the beam directions and the normal to iron plates ranging from 0° to 40°. A typical 500 MeV/c electron impinging at 0° and 40° is shown in fig. 4. The higher hit multiplicity in the YZ view is due to the fact that the Y-strips are placed orthogonally to the tubes. The distribution of the centroids of the clusters for the events in fig. 4 are shown in fig. 5. The number of hits in the XZ view and the energy resolution are shown as a function of energy in figs 6(a) and (b) for angles of 0° and 40°, respectively.

It is interesting to note that the energy resolution only changes by 25%.

The average number of hits in the YZ view is about twice that in the XZ view. The angular resolution for 0.5 GeV/c electrons impinging with angles of 0° and 40° is shown in fig. 7. A typical 0.5 GeV pion event and its centroid distribution are shown in figs 8 and 9, respectively. The difference in the features with respect to an electron event of the same energy (figs 4 and 5) is obvious.

Fig. 10 shows the range distribution for 300 MeV/c and 500 MeV/c π^-. The range is defined as the path length in iron of a single track up to the stopping point or a visible interaction with $\geqslant 2$ prongs.

For a 500 MeV/c π^-, 40% would be ambiguous with muons, and 5% with electrons. In these cases the muon and electron momenta will be generally different.

6. The neutrino run

The beam layout used in this run is shown in fig. 11 and described in sect. 3. The test module, placed im-

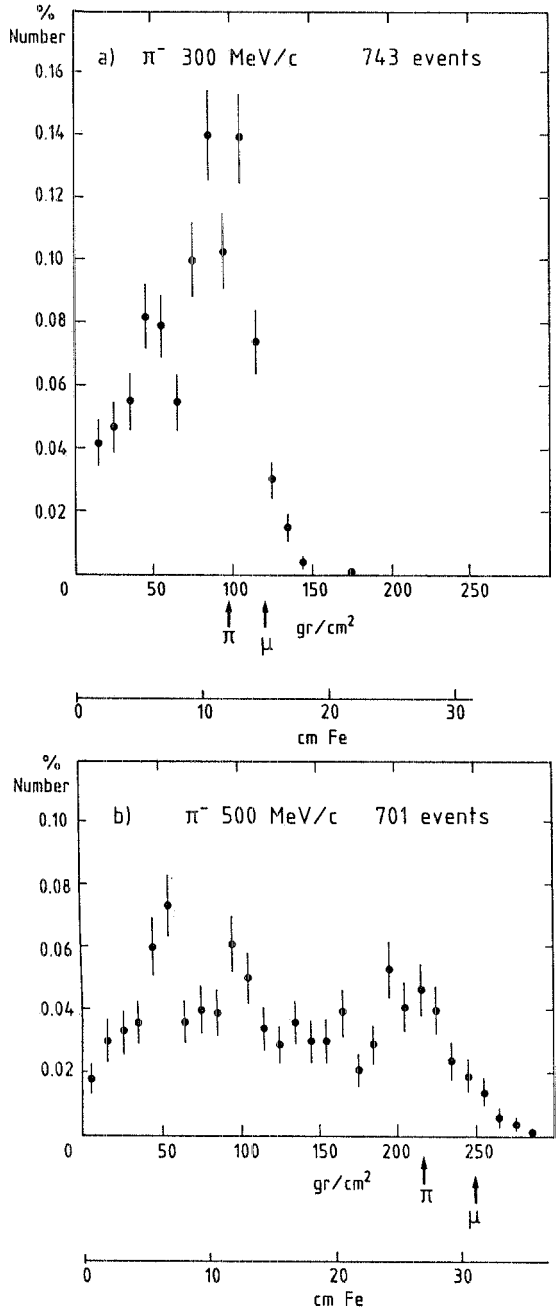

Fig. 10. Range distribution for 300 MeV/c and 500 MeV/c π^-.

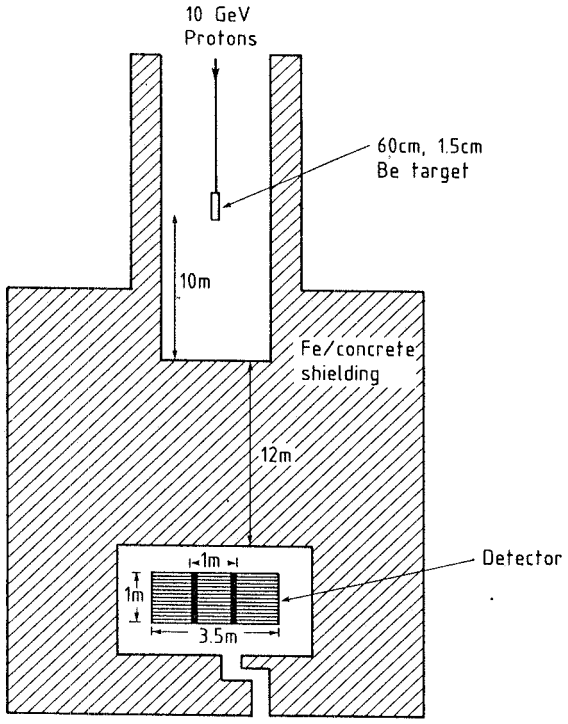

Schematic layout of neutrino beam used in the experiment.

Fig. 11. Schematic layout of the neutrino beam used in the experiment.

mediately behind the 12 m thick muon absorber, is heavily shielded in all directions with blocks of concrete to reduce the background of low energy neutrons.

The trigger system consists only in a gate opened by the beam signal for a time (2.5 μs) slightly exceeding the time width of the fast extracted proton beam incident on the target. This further reduces the background of slow neutrons produced around the proton target, which however still gives many single hits and sometimes even short tracks in the apparatus.

In order to simulate as well as possible the background of cosmic ray neutrinos in nucleon decay detectors two runs have been carried out with the detector axis placed at 0° and 45° with respect to the beam direction, with a total of 1.8×10^{18} and 1.5×10^{18} protons incident on target, respectively. The targetting efficiency varied considerably during the runs, with an average around 70%.

Candidates for neutrino interactions have been selected on the basis of the following criteria.

(a) at least three contiguous planes fire in the time gate;

(b) the vertex is contained between planes 3 and 25 and must be seen in both XZ and YZ view. This requirement gives a fiducial mass of ~ 2 t.

Events with two or more prongs are found to be uniformly distributed along the beam direction as expected for neutrino interactions. The same analysis for single prong events shows on the contrary that a fraction of events is distributed in an exponentially decreasing way, as expected for interactions of neutrons of a few hundreds of MeV/c producing in the detector pions and spallation protons which can cross more than two iron plates. In order to eliminate this background we

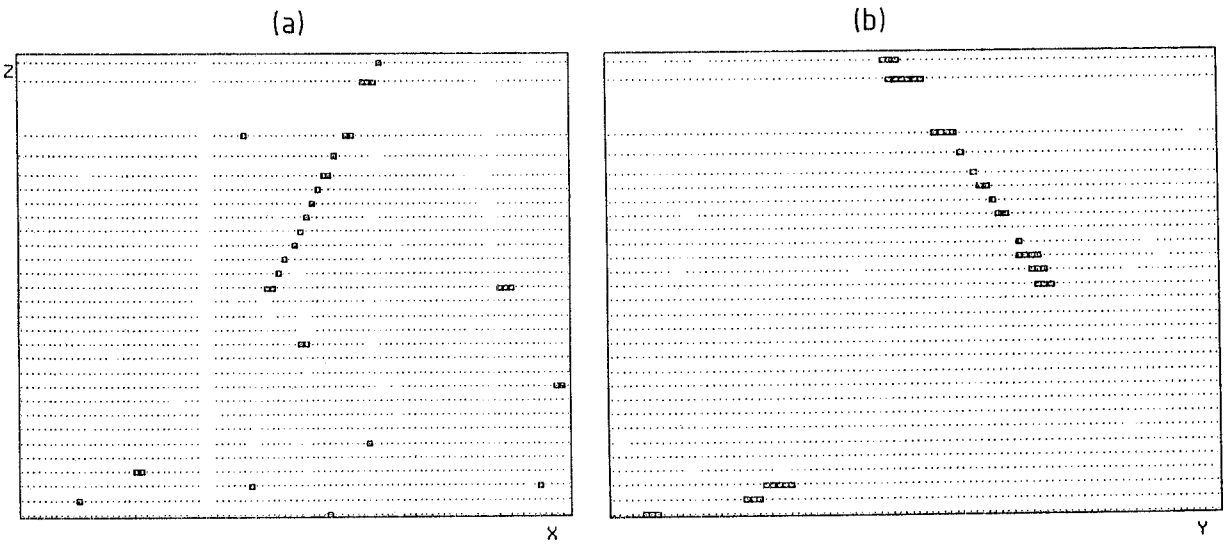

Fig. 12. A single prong neutrino event. (a) and (b) show the hits collected by XZ and YZ, respectively. The various small hits are due to the low energy neutron background.

Table 3
Experimental event distribution

	0°	45°
One prong	100	104
Two prongs	54	52
Three prongs	11	14
Four prongs	3	5
One prong + shower	11	7
Two prongs + shower	5	1
Neutral current candidate	23	13

have selected for further analysis only single prong events in which the track length exceeds a thickness of 10 cm of iron. This cut eliminated elastic charged current events with total energies below ~ 290 MeV and neutral current events consisting of a single pion or proton with kinetic energies below ~ 180 MeV and 340 MeV, respectively.

Two of the selected events are shown in figs. 12 and 13, while the total numbers in the various topologies are listed in table 3. The total numbers of events selected at

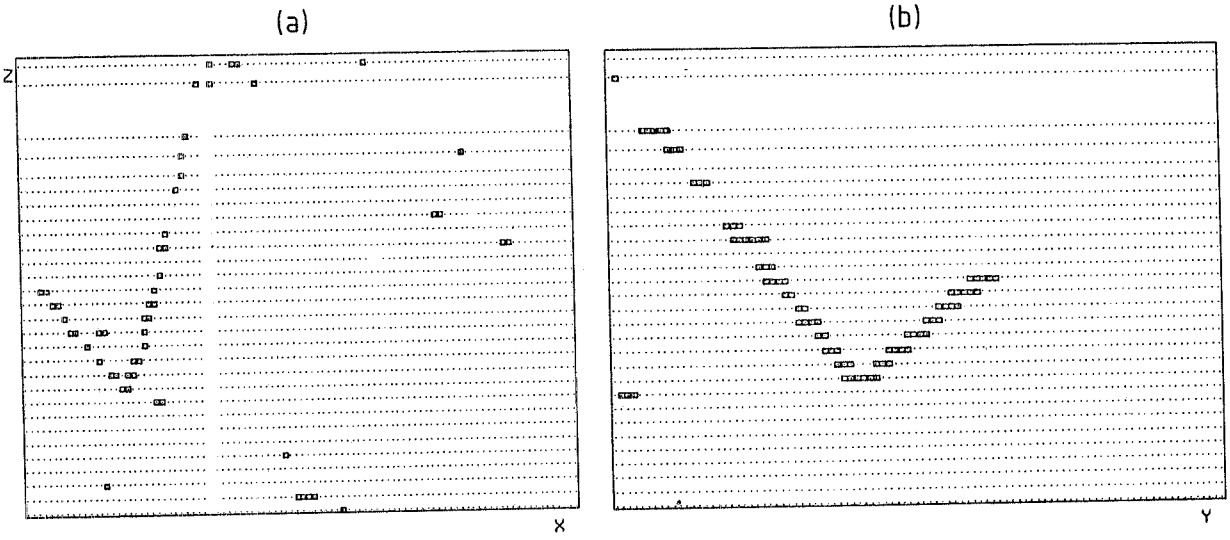

Fig. 13. A two-prong neutrino event. (a) and (b) as for fig. 12.

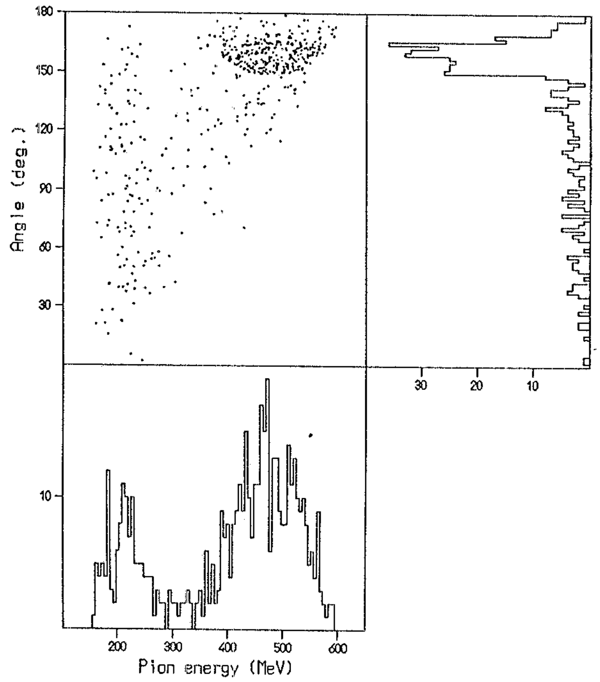

Fig. 14. Scatter plot of the pion total energy versus the opening angle for nucleon decays in iron, generated by Monte Carlo.

0° and 45° are 210 and 184, while the corresponding expected numbers are 260 ± 80 and 230 ± 70, respectively.

Note that in the event classification used for table 3 the knowledge of the neutrino direction was used. However, when considering these events as possible background for nucleon decay, we consider only the topology.

7. Evaluation of the neutrino background in nucleon decay experiments

Since these backgrounds are strongly dependent on the nucleon decay mode we will consider only a few specific channels:

(a) $\mu\pi$ or $e\pi$

(b) $n \to K^0\nu$, $K^0 \to \pi^+\pi^-$

(c) $p \to K^0\mu^+$, $K^0 \to \pi^+\pi^-$.

For events of type (a) we have performed a Monte Carlo calculation, which takes into account Fermi momentum and nuclear effects, to determine the angle between the lepton and the pion, and the pion energy, and the results are shown in fig. 14. We find that in 38% of the events the pion is absorbed, and of the remainder 25% have an opening angle $< 120°$.

In our test run we have scanned for two-prong events. The small size of the test detector means that in many cases a track leaves and therefore in these cases only a minimum energy estimate can be made.

Fig. 15 shows a scatter plot of the angle between the

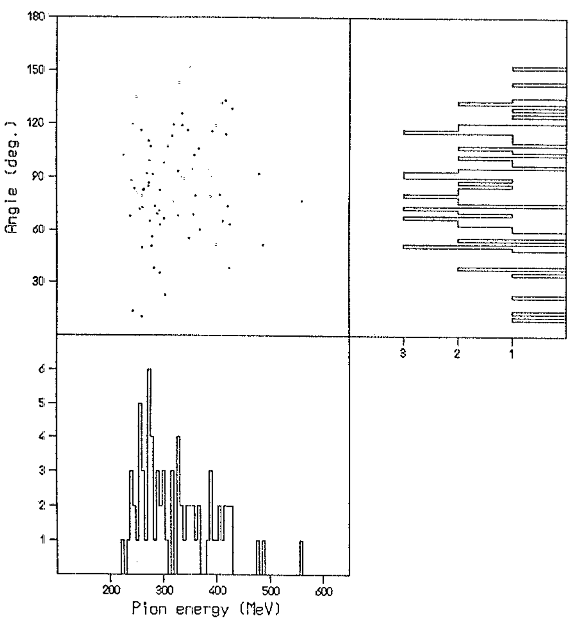

Fig. 15. The same plot as in fig. 14 for our two-prong neutrino events.

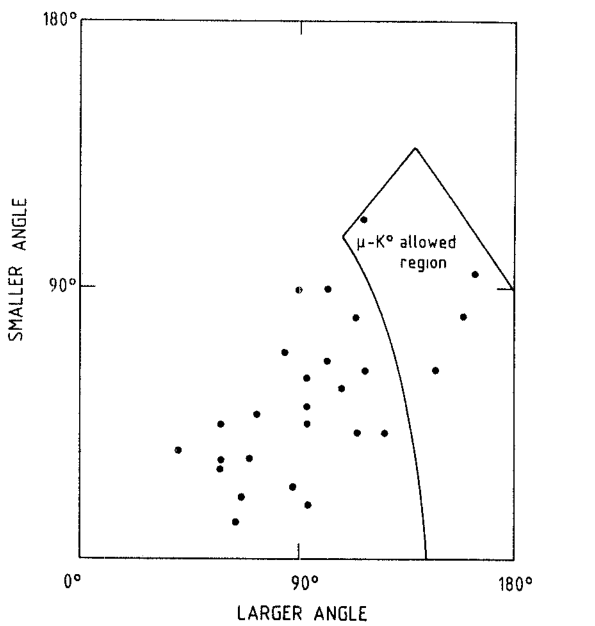

Fig. 16. Scatter plot in 3-prong ν events of the largest and smallest angles that the two other tracks make with the muon candidate.

lepton and the pion vs. pion energy, for the observed 2-prong events which have a visible total energy between 730 MeV and 1150 MeV. We observe 7 events with an angle $> 120°$; this in a total ν sample of 400 events. Hence the background simulating nucleon decay into a charged lepton and charged pion is $1.7 \pm 0.5\%$ of the atmospheric ν events.

We would like to stress that the background for the decay into lepton and π^0 is much lower. The reason for this is that in our data there are only 20% of 1 prong + shower, compared to 2-prong events. Only one of the 1-prong + shower events has an angle $> 120°$.

Events of type (b) would also appear as two-prong. Here nuclear effects are negligible. We have tried to fit all our two-prong events to the hypothesis $n \to K^0 \nu$ decay taking into account measurement error. We have found 11 events satisfying these conditions of which only two were not contained. In the case of non-contained events the energy of the leaving track was allowed to take energy above the minimum visible. The inclusion of these non-contained events will only slightly overestimate the background.

Therefore we conclude that the ν background to the $n \to K^0 \nu$ mode is $2.8 \pm 0.8\%$.

Events of type (c) will appear as 3-prong. Again in this mode nuclear effects are negligible.

We have observed 26, 3-prong events in our data, (25 charged currents plus 1 neutral current), and in fig. 16 we show a scatter plot of these events in terms of the largest and smallest angle which the muon candidate makes with respect to the two other tracks. Of the 4 events which lie in the region allowed for $p \to K^0 \mu$ decay (taking into account Fermi momentum) only 2 events have a minimum visible energy < 1.2 GeV.

Hence, at the most, only 0.5% of the ν_μ neutrinos interactions from the atmospheric neutrino flux will be a background in this channel, the ν_e flux being ineffective.

8. Conclusions

The present results can be applied to any proton decay calorimetric detector with the same density and granularity (1 cm spatial resolution in both views of each detector plane). In these conditions the maximum background from atmospheric ν's is at the 90% confidence level

(a) $e\pi$, $\mu\pi$, charged pion $< 2.7\%$
$e\pi$, $\mu\pi$, neutral pion $< 1.3\%$

(b) $n \to \nu K^0$
$\quad\quad \hookrightarrow \pi^+\pi^-, \quad < 4.4\%$

(c) $p \to \mu^+ K^0$
$\quad\quad \hookrightarrow \pi^+\pi^-, \quad < 0.80\%.$

As neutrino events occur at a rate of 0.16 ton · year, one third of which are due to ν_e, then our results show that the neutrino background will be equal to the decay rates, for the various topologies considered above, at lifetimes ranging from between 10^{32} and 10^{33} years in terms of lifetime/B.R. × efficiency for any set-up of this granularity to detect nucleon decay.

References

[1] For a recent review on this subject see for instance: H.H. Williams, Grand unification, proton decay, and neutrino oscillations, Talk presented at the SLAC Summer Institute on Particle Physics (August 16–24, 1982); and the Proc. of the 1983 Internat. Colloq. on Matter non-conservation held in Frascati (January 17–21, 1983) in press.
[2] J.L. Osborne, S.S. Said and A.W. Wonfendale, Proc. Phys. Soc. (London) B6 (1965) 93.
[3] M.R. Krishnaswami et al., Neutrino background in the Kolar Gold field nucleon decay experiment, to appear in PRAMANA.
[4] G. Battistoni et al., Phys. Lett. 118B (1982) 461.
[5] M.F. Crouch et al., Phys. Rev. D18 (1978) 2239.
[6] S. Barish et al., Phys. Rev. D16 (1977) 3103.
[7] G. Levman et al., Single charged current channels in ν–D_2 interactions, Topical Conf. on Neutrino Physics at Accelerators, Oxford (3–7 July 1978).
[8] S. Bonetti et al., Nuovo Cimento 38A (1977) 260.
[9] S. Barish et al., Phys. Lett. 66B (1977) 291.
[10] T. Eichen et al., Phys. Lett. 46B (1973) 274.
[11] N. Armenise et al., Nucl. Phys. 152B (1979) 365.
[12] T. Bolognese et al., Single pion production in $\bar{\nu}$ induced charged current interactions CERN/HE 78-26.
[13] E.C.M. Young, CERN 67-12 (1967).
[14] We are grateful to H. Wachmuth for discussions on this program and on the program DISMUNU.
[15] G. Battistoni et al., Proposal for an experiment on nucleon stability with a fine grain detector (December 1979) preprint.
[16] G. Battistoni et al., Nucl. Instr. and Meth. 202 (1982) 459.
[17] R. Barloutaud, talk given at ICOMAN-Bombay, (January 1982) PRAMANA in press.